UNMANNED SYSTEMS PAPER

Adaptive Fuzzy Sliding Mode Controller for the Kinematic Variables of an Underwater Vehicle

Eduardo Sebastián · Miguel A. Sotelo

Abstract This paper address the kinematic variables control problem for the low-speed manoeuvring of a low cost and underactuated underwater vehicle. Control of underwater vehicles is not simple, mainly due to the non-linear and coupled character of system equations, the lack of a precise model of vehicle dynamics and parameters, as well as the appearance of internal and external perturbations. The proposed methodology is an approach included in the control areas of non-linear feedback linearization, model-based and uncertainties consideration, making use of a pioneering algorithm in underwater vehicles. It is based on the fusion of a sliding mode controller and an adaptive fuzzy system, including the advantages of both systems. The main advantage of this methodology is that it relaxes the required knowledge of vehicle model, reducing the cost of its design. The described controller is part of a modular and simple 2D guidance and control architecture. The controller makes use of a semi-decoupled non-linear plant model of the Snorkel vehicle and it is compounded by three independent controllers, each one for the three controllable DOFs of the vehicle. The experimental results demonstrate the good performance of the proposed controller, within the constraints of the sensorial system and the uncertainty of vehicle theoretical models.

Keywords Adaptive equalization · Fuzzy models and estimators · Marine systems · Non-linear control · Robots dynamics · Sliding mode control

1 Introduction

Underwater vehicles have replaced human beings, in a great number of scenarios, especially in dangerous or precise tasks. Scientific and technological tasks, such as

E. Sebastián (✉)
Centro de Astrobiología (CAB), Laboratorio de Robótica y Exploración Planetaria,
Ctra. Ajalvir Km. 4. Torrejón de Ardoz, Madrid, Spain
e-mail: sebastianme@inta.es

M. A. Sotelo
Departamento de Electrónica, Universidad de Alcalá, N-II Km. 33. Alcalá de Henares, Madrid, Spain

underwater cave exploration, automatic sample recovery or cable and pipe inspection, make the design of automatic navigation and control systems necessary, giving the robot precision and autonomy. Even though the problem of underwater vehicle control is structurally similar to the control of a rigid body of six degrees of freedom (DOF), widely studied in the literature, it is more difficult because of the unknown non-linear hydrodynamic effects, parameter uncertainties, internal and external perturbations such us water current or sideslip effect.

The problem analysed in this paper, the low-speed control of the kinematic variables of an underactuated underwater vehicle, can be defined as follows. Given an unknown underwater vehicle plant and a continuous bounded time-varying velocity and/or position references, how to design a controller that ensures that the plant state converges asymptotically to the kinematic references. The designed controller is part of a control and guidance architecture, and it receives input references from the guidance system that ensures the tracking of the trajectory.

Most dynamically positioned marine vehicles in used today employ PI or PID controllers for each kinematic variable. These controllers are designed based on the assumption that the plant is a second order linear time invariant dynamical system, and that the disturbance terms of hydrodynamics forces, water currents and wind are constant. Additionally, they provide theoretically set point regulation if disturbances are constant, using Lasalle's Invariance Theorem, while they can not provide exact tracking even for linear plant [7]. Moreover, PID control can not dynamically compensate for unmodeled vehicle hydrody- namic forces or unknown variations in disturbances like current and wind. To avoid this problem only a reduced number of commercial vehicles employ model-based compensation of hydrodynamic terms and desired acceleration. The reason why these controllers are not widely used is that the required plant model is unavailable and the associated plant parameters are difficult to estimate with any accuracy, consequencely in practice they are empirically tuned by trial and error.

From this point of view, most of the proposed control schemes take into account the uncertainty in the model by resorting to an adaptive strategy or a robust approach. A significant number of studies have employed linearized plant approximations [13], in order to apply linear control techniques. In [18], a linear discrete time approximation for vehicle dynamics is used with reported numerical simulations of linear square and robust control methods. In [23] the author reports self-tuning control of linearized plant models and numerical simulations. In [20] the authors report linear model-reference adaptive control of linearized plant model and experimental demonstrations. In [19] the authors report the sliding-mode control of a linearized plant models and numerical simulations.

In the area of non-linear and modern control, relatively few studies directly address semi-decoupled non-linear plant models for underwater vehicles. In [33] the authors report non-linear sliding mode control for surge, sway and yaw movements. The most attractive characteristic of the sliding control is its inherent robustness to model uncertainties, obtained from an important control effort. Also, adaptive versions of sliding controllers have been implemented [10, 32], effectively reducing model uncertainty and control activity, and maintaining robustness without sacrificing performance. In [27] the authors compare, using experimental trial, some of the previously reported controllers, based on a decoupled non-linear plant model of the JHUROV vehicle.

Other techniques, besides sliding control have been used in UUV, in [16] a state linearization control is studied. However, this control technique can only be applied when the model of the system and its parameters are known. A step forward in the design of controllers with feedback linearization derives from the capacity to adapt the values of the

model parameters, supposing the model is known. In [9] an adaptive non-linear controller [26] has been tested, showing a practical implementation of a MIMO controller for the autonomous underwater vehicle AUV ODIN. One of the problems that this control law presents is the sensitivity to noise in the measurement of the kinematic variables. In [15] a modification of the non-linear adaptive control law is presented, in which during the process of adaptation the velocity and position measurements are replaced by their input references.

Several studies address fully coupled non-linear plant models and controllers [3, 4, 6] and [14]. In [21] a sliding control is used to stabilize the vehicle in a straight trajectory, considering model uncertainty and external perturbations. Other authors [1, 2] have taken into account the dynamics of the vehicle, for which they introduce the curvature of the trajectory like a new state variable. Lastly, in [12] the author gives a solution to the problem of the internal perturbations like the sideslip effect, or external like water currents, proposing an integrated methodology of guidance and control. For this, backstepping techniques are used which give a recursive design frame, guaranteeing the global stability by Lyapunov theory and accounting for the water currents by their estimation. Some of these approaches typically make explicit assumptions on the structure of the approximate vehicle plant dynamics to ensure that the vehicle plant model possesses passivity properties identical to those possessed by rigid-body holonomic mechanical systems, an assumption that has not been widely empirically validated for low speed underwater vehicles. In spite of that, the design of a unique controller for all the DOF of an underwater vehicle, in order to be part of a trajectory following system, is an area of research, still open [35]. At present, the motion and force control of the system vehicle-manipulator is one of the most active areas of research [5].

In the area of intelligent control, different controllers have been designed. For example, in [34] a neural control is proposed, using an adaptive recursive algorithm of which the principal characteristic is the on-line capability of adjustment, without having an implicit model of the vehicle, due to author employed nonparametric control methodologies that do not require knowledge of the plant dynamics. It has been tested with success in the ODIN vehicle. Finally, [11] proposes a fuzzy controller with 14 rules for depth control of an AUV.

This paper studies a kinematic variables controller, making use of a pioneering algorithm in underwater vehicles, which is based on the work and results developed in [31], about adaptive fuzzy sliding mode control (AFSM). The controller uses Euler angles and body fix reference frame to describe a semi-decoupled non-linear plant model of the underactuated Snorkel vehicle, that it is compounded by three independent controllers, each one for the controllable DOF. The methodology is an approach focused in the field of affine non-linear systems, based on uncertainty considerations, and model-based approximation of non-linear functions and feedback linearization with neural networks and fuzzy logic, [17] and [30]. The controller is based on the fusion of a sliding mode controller and an adaptive fuzzy system, adaptive exhibits and robust features. The adaptive capabilities are provided by several fuzzy estimators, while robustness is provided by the sliding control law, showing the advantages of both systems. But one of the main advantages of the proposed theory is that it employs a nonparametric adaptive technique which requires a minimum knowledge of plant dynamics, only needing a theoretical and simple model. A Lyapunov-like stability analysis of the control algorithm is described. The algorithm is also based on the analysis developed in [31], which has been adapted to the peculiarities of the vehicle model, with some changes. The stability analysis ensures the stability of the adaptation process and the convergence to the references. The resulting control law is validated in practical experiments for controlling the Snorkel, carried out for the first time in this work, by a

UUV developed at the Centro de Astrobilogía. The most important characteristic of the vehicle is the low cost of all instruments and methods used in the design, conditioning and limiting the identification experiments.

Additionally, the paper reports a direct comparison of the performance of the AFSM controller with more simple control schemes like sliding mode controller (SM) or a velocity PI controller, based on a theoretical plant model and investigating the effects of bad model parameters on system tracking performance. Practical aspects of the implementation are also discussed. The experimental results obtained demonstrate the good performance of the proposed controller, outperforming more simple ones.

The paper is organized as follows; Section 2 introduces the dynamic equations of underwater robots, specified for the Snorkel vehicle, as well as the vehicle control and guidance architecture. In Section 3 the AFSM controller and its theoretical demonstrations of stability are presented, additionally, more simple SM or PI controllers are analyzed too. Section 4 is dedicated to the experiments setup, and Section 5 presents a series of real experiment results and the performance of the controllers is described and compared. Finally, Section 6 summarizes the results.

2 Dynamical Modelling and Vehicle Architecture

Finite dimensional approximate plant models for the dynamics of underwater vehicles are structurally similar to the equations of motion for fully actuated holonomic rigid-body mechanical systems, in which plant parameters enter linearly into the non-linear differential equations of motion.

In this work a Newton–Euler formulation and a non-inertial reference system have been selected, as the method to obtain the dynamic model of an underwater vehicle; Eq. 1. Euler angles representation has been chosen despite the presentation of singularities. General underwater vehicles, such us Snorkel, shows moderate pitch and roll motion;[1] thus there are not physically attained values to cause singularities representation of the vehicles orientation. Considering the marine vehicle shown in Fig. 1, its most reported finite dimensional model responds to non-linear dynamic equations of 6-DOF, that can be represented in compact form (including vehicle thruster forces, hydrodynamic damping, and lift and restoring forces) with the equation [14],

$$M\dot{v} + C(v)v + D(v)v + g(\eta) = \tau, \tag{1}$$

where $M \in \Re^{6\times6}$ mass matrix that includes rigid body and added mass and satisfies $M = M^T > O$ and $\dot{M} = 0$; $C(v) \in \Re^{6\times6}$ matrix of Coriolis and centrifugal terms including added mass and satisfies $C(v) = -C(v)^T$; $D(v)v \in \Re^{6\times6}$ matrix of friction and hydrodynamic damping terms; $g(\eta) \in \Re^6$ vector of gravitational and buoyancy generalized forces; $\eta \in \Re^3$ is the vector of Euler angles; $v \in \Re^6$ is the vector of vehicle velocities in its six DOF, relative to the fluid and in a body-fixed reference frame and $\tau \in \Re^6$ is the driver vector considering vehicle thrusters position.

Actually there is no an exact model to describe the value of some of these matrix and vectors (1). A rigorous analysis would require the implementation of the Navier–Stokes

---

[1]The metacentric height, or the distance between the centre of buoyancy and the centre of mass, is high enough to ensure the static stability of the vehicle in pitch and roll movements.
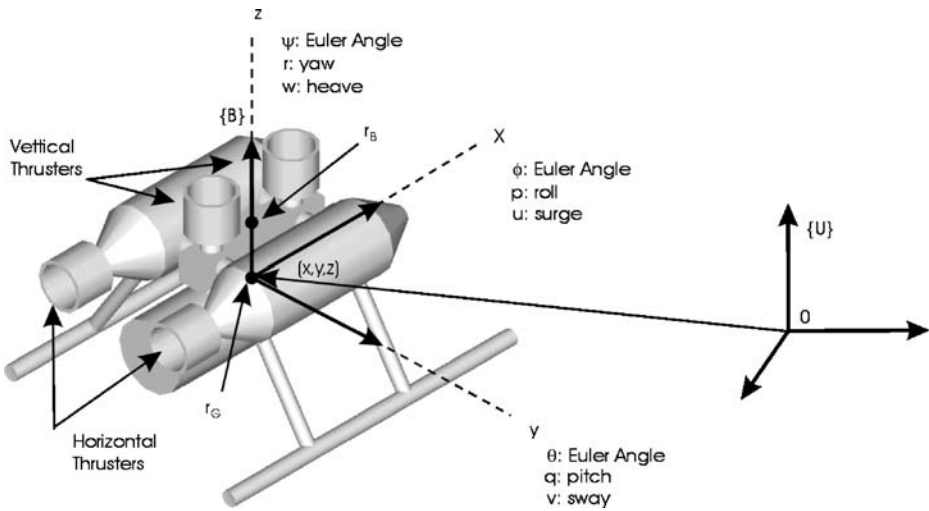
Fig. 1 Frames and elementary motions of the vehicle

equations (distributed fluid-flow) which are rather complex to implement and also make the development of reliable models difficult for most of the hydrodynamic effects. In this paper, we are only interested in those physical phenomena which significantly affect the dynamic properties of the vehicle under consideration. In this context, the modelling of the hydrodynamic effects is considered. Although not completely justified, the common practice [14] to simplify the vehicle model is adopted which considers null values for: off diagonal entries of the damping matrix $D(v)$, with only linear and/or square terms, inertial products and the tethered dynamics, as well as assuming a constant added mass. From this point of view, the Eq. 1 can be simplified [27] and divided in each of the semi-decoupled single DOF equations, taking the form (2). Despite the fact that the model can be represented separately for each DOF, it is coupled due to the Coriolis and centripetal terms, as well as the buoyancy and weight, which depend on the vehicle velocities and angles in other DOF.

$$\tau_i = m_i \ddot{x}_i + c_i(v) + X_{|\dot{x}_i|\dot{x}_i} |\dot{x}_i| \dot{x}_i + g_i(\eta) + d_i(t), \tag{2}$$

where, for each DOF i, τ_i *is the control force or moment,* m_i *is the effective inertia,* $c_i(v)$ *are the Coriolis and centripetal terms,* $X_{|\dot{x}_i|\dot{x}_i}$ *is the square hydrodynamic drag coefficient,* $g_i(\eta)$ *is the buoyancy and weight term,* d_i *is a term that represents unmodeled dynamics and perturbations, and* $\dot{x}_i$ *and* $\ddot{x}_i$ *are the velocity and acceleration of the vehicle in the body reference frame.* Or in other words,

$$\ddot{x}_i = f_i(\xi) + g_i(\xi)\tau_i \tag{3}$$

where $f_i(\xi) = \frac{1}{m_i} \left[-c_i(v) - X_{|\dot{x}_i|\dot{x}_i} |\dot{x}_i| \dot{x}_i - g_i(\eta) - d_i \right]$ and $g_i(\xi) = 1/m_i$.

We used the nomenclature convention described in Table 1. Lineal position, as well as vehicle velocity and acceleration, are given with respect to the body-coordinate frame. Note that the velocity in inertial coordinates is related to the velocity in the body frame by a non-linear transformation, in which the Euler angles take part.

Table 1 Nomenclature

DOF	Surge	Sway	Heave	Yaw	Pitch	Roll
Force/moment	τ_u [N]		τ_w [N]			τ_r [Nm]
Velocities	$\dot{x}_u$ [m/s]	$\dot{x}_v$ [m/s]	$\dot{x}_w$ [m/s]	$\dot{x}_p$ [rad/s]	$\dot{x}_q$ [rad/s]	$\dot{x}_r$ [rad/s]
Positions/angles	x_u [m]	x_v [m]	x_w [m]	x_p [rad]	x_q [rad]	x_r [rad]

2.1 Control and Guidance Architecture

The kinematic variables controller described in this paper is part of a control and guidance architecture, dedicated to achieve the local and autonomous navigation. The goal of the navigation algorithm is to maintain an adequate distance from walls and objects, and to be parallel to them. These trajectories agree with the scientific tasks of the vehicle in an unknown and remote environment. From this point of view local navigation was selected because exact global position was not required, helping to reduce the cost of the inertial sensors, which is one of the main objectives of the vehicle designers. The architecture uses the local character information (local position d_e and angular ψ_e errors) extracted from the environment by a Forward Looking Sonar image (FLS), due to the intrinsic difficulties associated with underwater global positioning in unknown and abrupt environments [28].

The control and guidance architecture is based on three chained controllers. Each controller's goal is to generalize the system dynamics for their use by the controllers at a higher hierarchical level [13], reaching in this way the autonomous following of the trajectory defined by the navigation system. The closest controller to vehicle hardware is that of propulsion. It receives thrust input references from the kinematic variables controller, of higher hierarchical level, and generates voltage values to be applied to the motors of the thrusters. The kinematic variables controller is in charge of following the kinematic references (surge and yaw velocities) given by the guidance system, and (heave position) given by the reference generator of the navigation system. Finally, the highest hierarchical controller is the guidance system, which is dedicated to the carrying out of local trajectory tracking in a horizontal plane, taking into account the effect of water currents and sideslip [25]. The controller makes null the values of the trajectory following errors, d_e and ψ_e, which are not measured by the integration of angular and linear velocities, on the contrary, they are estimated from the analysis of the FLS image. In Fig. 2, a diagram of the control architecture, with the nomenclature criteria of Table 1, is shown.

3 Fuzzy Sliding Mode Control Algorithm

In this section the equations and a stability analysis of the resulting close loop of the AFSM controller are presented. Additionally, these characteristics are also studied by a simple PI controller and a model based SM controller. The controllers have been designed to track position and velocity references for the surge, heave and yaw movements.

3.1 Velocity PI Controller (PI)

The basic velocity PI controller for a single-DOF plant takes the form.

$$\tau = K_i \widetilde{x} + K_p \dot{\widetilde{x}}, \tag{4}$$
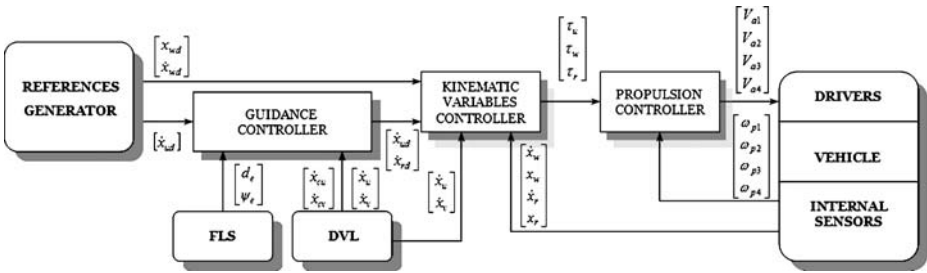
Fig. 2 Control architecture diagram

where K_i and K_p are scalar error feedback gains. The state error coordinates are defined as

$$\widetilde{x} = x - x_d, \quad \dot{\widetilde{x}} = \dot{x} - \dot{x}_d, \tag{5}$$

where x_d and $\dot{x}_d$ are the desired position and velocity, and x and $\dot{x}$ are the actual plant position and velocity. Substituting Eq. 4 into Eq. 2, the resulting closed-loop dynamical system is

$$0 = m\ddot{x} + c(\boldsymbol{v}) + X_{|\dot{x}|\dot{x}}|\dot{x}|\dot{x} + g(\boldsymbol{\eta}) + d_i - K_i\widetilde{x} - K_p\dot{\widetilde{x}}. \tag{6}$$

It is necessary to emphasize that when position references are used, the PI controller behaves more like a PD controller. In the case where the buoyancy term $g(\boldsymbol{\eta})+d_i$ is zero, the PI controller will perform set point regulation, but not trajectory tracking [27]. In spite of the fact that the PI controller does not reach good performance, it represents the most widely used controller in use in the world, and therefore it represents a baseline on which to compare the performances of our controller.

3.2 Model-based Sliding Mode Controller (SM)

The SM controller for a single DOF takes the form

$$\tau = \widehat{g}(\xi)^{-1}\left[\widehat{f}(\xi) - \lambda\dot{\widetilde{x}} + \ddot{x}_d - \eta_\Delta \mathrm{sat}(s/b)\right], \tag{7}$$

where $\widehat{g}(\xi)$ and $\widehat{f}(\xi)$ are the estimation of the $g(\xi)$ and $f(\xi)$ system function respectively due to the fact that these functions are not completely known for the Snorkel vehicle, λ, b and η_Δ are positive definite constant, and the sliding surface is defined as $s = \dot{\widetilde{x}} + \lambda\widetilde{x}$.

The evolution of the sliding mode controller can be divided in two phases, Fig. 3: The approximation phase, where $s\neq0$, and the sliding phase when $s=0$. The right election of the parameter η_Δ, based on the uncertainty boundaries of system functions and perturbations, allows the designer to ensure that error vectors $\dot{\widetilde{x}}$ and $\widetilde{x}$ change from the approximation phase to the sliding phase. Once on the surface or in the sliding phase, it is ensured that the system follows the input references, in presence of uncertainties, with a time constant of value, $\frac{1}{\lambda}$. The saturation function is used to avoid the chattering effect [26].

The Lyapunov candidate function V [26] is chosen to analyze if the control law (7) is stable, and to determine the values of η_Δ that make all the signals remain bounded.

$$V = \frac{1}{2}\left[s_i^2\right], \tag{8}$$
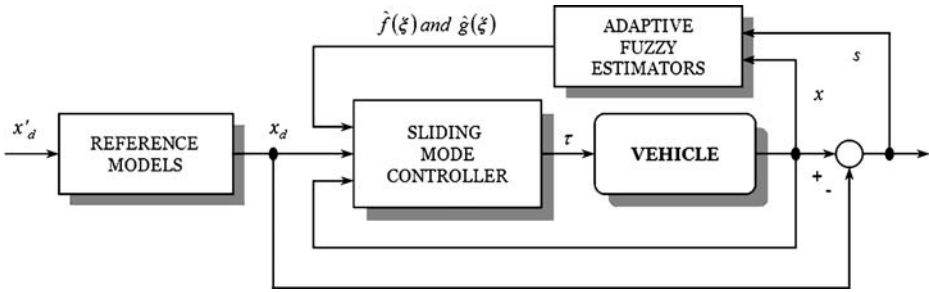
Fig. 3 Adaptive fuzzy sliding mode controller diagram

If the Lyapunov condition $s\dot{s} \leq \eta|s|$ is applied, where η is a positive constant, the derivative will be $\dot{V} \leq 0$. Thus, from the definition of the sliding surface and expressions (3) and (7), and for positive values of s all of them bigger than their respective b, this means that $\dot{s} \leq \eta$. And solving for η_Δ yields,

$$\eta_\Delta \geq \eta + \left[\frac{\widehat{g}(\xi)}{g(\xi)}f(\xi) - \widehat{f}(\xi)\right] + \left[\ddot{x}_d - \frac{\widehat{g}(\xi)}{g(\xi)}\ddot{x}_d\right] + \left[\frac{\widehat{g}(\xi)}{g(\xi)}\lambda\dot{\widetilde{x}} - \lambda\dot{\widetilde{x}}\right] + \frac{\widehat{g}(\xi)}{g(\xi)}d \qquad (9)$$

As can be seen in Eq. 9 that the value of η_Δ depends on the choice of another parameter η, which at the same time is defined by T, or the time that the state vector spends in reaching the sliding condition. The mathematical interpretation of this parameter, for positive values of s, is $T \leq \frac{s_0}{\eta}$.

To summarize, all the signals remain bounded, and the velocity error asymptotically tracks to zero. This approach is an application to underwater vehicles of the general methodology reported in [26].

3.3 Adaptive Fuzzy Sliding Mode Controller (AFSM)

The AFSM controller shares the control law for a single DOF with the SM controller (7). In this case, since functions $f(\xi)$ and $g(\xi)$ of the vehicle model are partially unknown and non-linear, a set of fuzzy functions to estimate them is proposed, being the control diagram of the overall system shown in the Fig. 3.

3.3.1 Fuzzy Adaptive System

A fuzzy system may be used like a non-linear universal approximator [30], due to its ability to introduce verbal information from the previous knowledge of an operator, and its capacity to uniformly approximate any real and continuous function with different degrees of precision. In general, good verbal information can help to establish initial conditions, and so faster adaptation will take place.

Any fuzzy system is a collection of IF-THEN rules of the form: $R^{(j)}$: IF x_1 is A_1^j and ... and x_n is A_n^j THEN y is B^j. By using a Sugeno-like fuzzy system, Fig. 4, with a singleton fuzzification strategy, product interface and media defuzzification, the fuzzy system output is,

$$y(\xi) = \boldsymbol{\theta}^T \boldsymbol{\zeta}(\xi) \qquad (10)$$

where $\boldsymbol{\theta} = (y^1, \ldots, y^m)^T$, $\quad \boldsymbol{\zeta}(\xi) = \left(\zeta^1(\xi), \ldots, \zeta^m(\xi)\right)^T$ with $\zeta^j(\xi) = \frac{\prod_{i=1}^{n}\mu_{A_i^j}(\xi_i)}{\sum_{j=1}^{m}\left[\prod_{i=1}^{n}\mu_{A_i^j}(\xi_i)\right]}$, $\mu_{A_i^j}(\xi_i)$ are
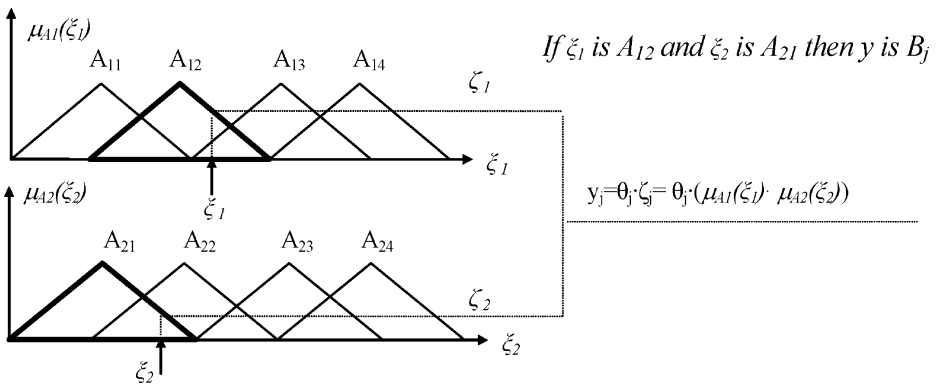
Fig. 4 Sugeno-like fuzzy system diagram

the membership functions of the fuzzy variable ξ_i, and y^j is the point in R in which μ_{Bj} achieves its maximum value, that is $\mu_{Bj}(y^j) = 1$. Thus the functions $f(\xi)$ and $g(\xi)$ are parameterized by fuzzy logic systems as,

$$\widehat{f}(\xi|\theta_f) = \theta_f^T \zeta(\xi), \quad \widehat{g}(\xi|\theta_g) = \theta_g^T \zeta(\xi), \tag{11}$$

where $\zeta(\xi)$ is supposed to be fixed, while the elements θ_f^T and θ_g^T can be adaptatively tuned till they reach the optimal values, θ_f^* and θ_g^*.

3.3.2 Adaptation Law

The adaptive functions will be tuned by the next parameter adaptation algorithm [31],

$$\sum\nolimits_1 : \dot{\theta}_f = \begin{cases} r_1 s \zeta(\xi) & \text{if} \quad \left(|\theta_f| < M_f\right) \text{ or } \left(|\theta_f| = M_f \text{ and } s\theta_f^T\zeta(\xi) \leq 0\right) \\ P\{r_1 s \zeta(\xi)\} & \text{if} \quad \left(|\theta_f| = M_f \text{ and } s\theta_f^T\zeta(\xi) > 0\right) \end{cases} \tag{12a}$$

$$\sum\nolimits_2 : \dot{\theta}_g\big|_{\theta_{gj}>\in} = \begin{cases} r_2 s \zeta(\xi)\tau & \text{if} \quad \left(|\theta_g| < M_g\right) \text{ or } \left(|\theta_g| = M_g \text{ and } s\theta_g^T\zeta(\xi)\tau \leq 0\right) \\ P\{r_2 s \zeta(\xi)\tau\} & \text{if} \quad \left(|\theta_g| = M_g \text{ and } s\theta_g^T\zeta(\xi)\tau > 0\right) \end{cases} \tag{12b}$$

$$\sum\nolimits_3 : \dot{\theta}_{gj}\big|_{\theta_{gj}=\in} = \begin{cases} r_2 s \zeta_j(\xi)\tau & \text{if} \quad s\zeta_j(\xi)\tau > 0 \\ 0 & \text{if} \quad s\zeta_j(\xi)\tau \leq 0 \end{cases} \tag{12c}$$

where r_1, r_2 are positive constants that define adaptation velocity, M_f, M_g are positive constants that fix the maximum value of second norm of θ_f and θ_g respectively, and $\in$ specifies the minimum value of the elements of θ_g, $\zeta_j(\xi)$ is the jth element of $\zeta(\xi)$, θ_{gj} is the jth element of θ_g, s and τ are the values of the sliding surface and the control action, and the projection operators $P\{*\}$ are defined as $P\{r_1 s\zeta(\xi)\} = r_1 s\zeta(\xi) - r_1 s \frac{\theta_f \theta_f^T \zeta(\xi)}{|\theta_f|^2}$ and $P\{r_2 s\zeta(\xi)u\} = r_2 s\zeta(\xi)\tau - r_2 s \frac{\theta_g \theta_g^T \zeta(\xi)\tau}{|\theta_g|^2}$.

Theorem [34] *For a non-linear system* (3), *consider the controller* (7). *If the parameter adaptation algorithm* (12a, 12b *and* 12c) *is applied, then the system can guarantee that:* (a) *the parameters are bounded, and* (b) *closed loop signals are bounded and tracking error converges asymptotically to zero under the assumption of a fuzzy integrable approximation error.*

Proof. Boundedness of θ_f and θ_g By considering the adaptation algorithm for θ_f, the Lyapunov candidate function $V_f = \frac{1}{2}\theta_f^T\theta_f$ is chosen. If the first line of Eq. 12a is true, then if $|\theta_f|<M_f$ and $\dot{V}_f = r_1 s\, \theta_f^T\zeta(\xi) \le 0$, but if $|\theta_f|=M_f$ then $|\theta_f|\le M_f$ always. If the second line of Eq. 12a is true, then $|\theta_f|=M_f$ and $\dot{V}_f = r_1 s\, \theta_f^T\zeta(\xi) - r_1 s \frac{|\theta_f|^2\theta_f^T\zeta(\xi)}{|\theta_f|^2} = 0$ that is $|\theta_f|\le M_f$. To sum up, $\left|\theta_f(t)\right| \le M_f \quad \forall t > 0$ is guaranteed. In the same way $\left|\theta_g(t)\right| \le M_g \quad \forall t > 0$ can be proved.

The proof of $\theta_{gj}\ge\in$ may be shown as follows, from Eq. 12c if $\theta_{gj}=\in$ then $\dot{\theta}_{gj}\ge 0$, which implies that $\theta_{gj}\ge\in$ for all elements θ_{gj} of θ_g, and this guarantees that the controller (6) can be constructed.

Proof. Boundedness of s and stability analysis Define the minimum approximation error $\omega = f(\xi) - \widehat{f}(\xi|\theta_f^*) + (g(\xi) - \widehat{g}(\xi|\theta_g^*))\tau$, and assuming that η_Δ is the parameter to meet the sliding mode control law (9). From Eqs. 3 and 7 $\dot{s} = \widehat{f}(\xi|\theta_f^*) - \widehat{f}(\xi|\theta_f) + (\widehat{g}(\xi|\theta_g^*) - \widehat{g}(\xi|\theta_g))\tau + d + \omega - \eta_\Delta\mathrm{sat}(s/b)$, can be shown, in other words,

$$\dot{s} = \widetilde{\theta}_f^T\zeta(\xi) + \widetilde{\theta}_g^T\zeta(\xi) + d + \omega - \eta_\Delta\mathrm{sat}(s/b), \tag{13}$$

where $\widetilde{\theta}_f = \theta_f^* - \theta_f$ and $\widetilde{\theta}_g = \theta_g^* - \theta_g$.

Considering the Lyapunov candidate function,

$$V = \frac{1}{2}\left[s^2 + \frac{1}{r_1}\widetilde{\theta}_f^T\, \widetilde{\theta}_f + \frac{1}{r_2}\widetilde{\theta}_g^T\, \widetilde{\theta}_g\right], \tag{14}$$

the derivative of V can easily be shown to be,

$$\dot{V} = s\dot{s} + \frac{1}{r_1}\widetilde{\theta}_f^T\, \dot{\widetilde{\theta}}_f + \frac{1}{r_2}\widetilde{\theta}_g^T\, \dot{\widetilde{\theta}}_g \tag{15a}$$

$$\dot{V} \le s\omega + I_1 s\frac{\widetilde{\theta}_f^T\theta_f\, \theta_f^T\zeta(\xi)}{\left|\theta_f\right|^T} + I_2 s\frac{\widetilde{\theta}_{g+}^T\theta_{g+}\theta_+^T\zeta_+(\xi)\tau}{\left|\theta_{g+}\right|^T} + I_3\widetilde{\theta}_{g\in}^T\zeta_\in(\xi)s\,\tau \tag{15b}$$

where $I_{1,2,3} = \begin{cases} 0, \text{ If the first line of adaptation algorithm is true} \\ 1, \text{ If the second line of adaptation algorithm is true} \end{cases}$, θ_{g+} denotes the set of $\theta_{gj}>\in$, $\theta_{g\in}$ denotes the set of $\theta_{gj}=\in$, $\widetilde{\theta}_{g+} = \theta_{g+} - \theta_{g+}^*$, $\widetilde{\theta}_{g\in} = \theta_{g\in} - \theta_{g\in}^*$, $\zeta_+(\xi)$ and $\zeta_\in(\xi)$ are the basic function sets corresponding to θ_{g+} and $\theta_{g\in}$ respectively.

It is necessary to prove that the terms I_1, I_2 in Eq. 15b are non positives and I_3 is non negative. For $I_1 = 1$ this means $|\theta_f|=M_f$ and $s\,\theta_f^T\zeta(\xi) > 0$, since $|\theta_f| = M_f\ge|\theta_f^*|$ then $\widetilde{\theta}_f^T\theta_f = \left(\theta_f^* - \theta_f\right)^T\theta_f = \frac{1}{2}[|\theta_f^*|^2 - |\theta_f|^2 + |\theta_f^* - \theta_f|^2] \le 0$. Therefore the terms I_1 are non positives. Following the same procedure, the terms I_2 can be proved to be non positives too. In the case $I_3=1$ and based on Eq. 15b and $\widetilde{\theta}_{g\in} = \theta_{g\in}^* - \in > 0$, it can be proved that the terms I_3 are non negative. Thus, this means $\dot{V} \le s\omega$. Applying the universal approximation theorem, it can be expected that the term $s\omega$ is very small or equal to zero [31]. This implies $\dot{V} \le 0$.

It can be concluded that s, $\boldsymbol{\theta}_f$ and $\boldsymbol{\theta}_g$ are bounded, thus if the reference signal x_d is bounded, the system state variable x will be bounded, and that both the velocity tracking error and the time derivative of the parameter estimates converge asymptotically to zero. However, in the absence of additional arguments, it can not be claimed either $\lim_{t\to\infty} |x(t)| = 0$, $\lim_{t\to\infty} |s(t)| = 0$ or that $\lim_{t\to\infty} \left|\tilde{\boldsymbol{\theta}}_f\right| = 0$ and $\lim_{t\to\infty} \left|\tilde{\boldsymbol{\theta}}_g\right| = 0$. This approach is the application, for the very first time, to underwater vehicles of the general methodology originally reported in [31].

4 Experimental Setup

4.1 The Snorkel Vehicle

The Snorkel vehicle, shown in Fig. 5, is a reduced cost remotely operated UUV. The main goal of the vehicle is to carry out a scientific and autonomous inspection task in the Tinto River. The Tinto River is an unknown and remote environment, whose geological and biological characteristics are causing increased astrobiological interest, due to it being host to a great variety of extremophile microorganisms with a quimiolitrotophical origin. The Snorkel vehicle is powered by a 300 W AC power supply. The dry mass of the vehicle is 75 kg and its dimensions are 0.7 m long×0.5 m wide and 0.5 m high. The vehicle is passively stable in the roll and pitch angles. Actuation is provided by four DC electric motors, two of them are placed in a horizontal plane while the others are in a vertical one.

The electronics architecture of the Snorkel vehicle has been designed ad hoc and is based on a distributed system. It uses two different communication buses; a deterministic CAN bus inside the vehicle and an Ethernet bus to link the robot with the surface and the teleportation station. The main vehicle CPU is compound by a PC104 board with a Pentium-III at 600 MHz and the RT-Linux operative system. It hosts the control algorithms described in this paper, so a digital version of them with an Euler integration algorithm and a sample period of 100 ms have been used. The rest of the nodes of the bus are compounded by HCS12 microcontrollers, which are dedicated to a sensors interface and thrusters control. A complete description of this architecture is reported in [25].

Fig. 5 Snorkel robot image
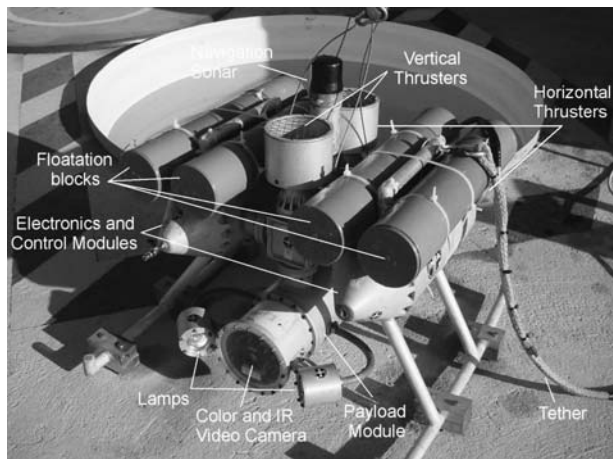
The Snorkel vehicle is tethered, and despite the umbilical cable, can play an important role in the dynamics of a small underwater vehicle, there are several reasons that allow as to think that in this specific application this issue is not going to represent an important problem, simplifying the design of the whole system: First, because of the reduced cable dimensions and its neutral buoyancy, with 12 mm of diameter and a length smaller than 120 m. This is due to the small lake dimensions, and the ad hoc design of the cable with power line modem communications with the surface. Second, because there is almost a complete absence of water currents in the lake, which also reduces the influence of the umbilical cable. And finally, because of the characteristics of the proposed controller, which adapts the dynamics of the umbilical cable, so that it would be part of the vehicle dynamics. This characteristic can be also seen as an advantage of the proposed controller.

The Snorkel vehicle is equipped with a low cost sensorial system. There is a set of three ENV-05D gyroscopes of the company Murata to measure the vehicle angular velocities, an inclinometer to obtain the value of roll and pitch angles and a compass for the heading, all of them integrated in the digital system HMR3000 of Honeywell. Depth is instrumented via a 600 kPa BOSCH pressure sensor, additionally the pressure output signal is differentiated to obtain a simple measure of the heave velocity. Finally, it is necessary to point out that a lineal velocity measurement system is implemented by using the Doppler Velocity Log system (DVL) of the company Sontek. The quality of all sensor output is not enough for making an inertial navigation, thus a drift in the estimation of the vehicle position is generated as a result of the integration of these signals. The vehicle's sensors and its characteristics are listed in Table 2.

4.2 Implementation Issues

The experiments have been carried out in a small tank of 1.8 m of diameter and 2 m of depth, the small size of which can affect vehicle dynamics. Based on these limits and trying to avoid bumping with tank walls, the close loop tests only study the controller behaviour in yaw and heave movements. However, the results can be extended to the surge DOF. Trials were conducted tracking square position and velocity references, both magnitudes are expressed in the body coordinates. Additionally, while an experiment is made in one DOF, the references for the rest of the two controllable DOF are zero.

Based on the robustness and adaptability properties of the proposed control law, it is only necessary to have a theoretical estimation of the parameters which determine the semi-decoupled single DOF dynamic model of the Snorkel vehicle (2). In [25] the set of plant parameters are obtained for the 6 DOF of the vehicle, using theoretical and simplified theories of vehicle dynamics. For example the strip theory has been used to determine the

Table 2 Vehicle instrumentation

Variable	Sensor	Precision	Update rate
Angular velocity	ENV-05D gyroscopes	0.14°/s	100 ms
Depth	600 kPa pressure sensor	5 cm	100 ms
Heave velocity	Differential presume	1 cm/s	100 ms
Roll, pitch and yaw	HMR3000	0.1°	50 ms
Heave, surge and sway	Sontek DVL	1 mm	100 ms

Table 3 Theoretical vehicle parameters

DOF	Inertia (m_i)	Coriolis-centripetal (c_i)	Square damping ($X_{|ui|ui}$)	Buoyancy
Surge	82.5 [kg]	$226\dot{x}_v \cdot \dot{x}_r$ [kg·m/s^2]	100 [N/(m/s)^2]	0 [N]
Heave	226 [kg]	0 [kg·m/s^2]	215.25 [N/(m/s)^2]	0 [N]
Yaw	10.84 [kg·m^2]	$133.5 \cdot \dot{x}_u \cdot \dot{x}_v$[kg·m^4/s^2]	9 [N·m/(rad/s)^2]	0 [N·m]

added mass coefficients, and Morrison equation for hydrodynamic damping [14]. In Table 3, a summary of these parameters for the three controllable DOF can be seen.

The relationship between the force/moment acting on the vehicle $\boldsymbol{\tau} \in \Re^6$ and the control input of the four thrusters of the Snorkel vehicle, Fig. 1, $\boldsymbol{u} \in \Re^4$ is highly non-linear. Generally, thrusters are the main cause of limit cycle in vehicle positioning and bandwide constraint. A simplified and static thrust model has been used for these tests. The control action in each DOF, force or moment, is divided between the two thrusters associated to that DOF, Fig. 1. The force generated by the thruster is assumed to follow a square input–output relation between propeller velocity and thrust, $\tau_i = C_\tau \omega_p |\omega_p|$, where C_τ is an experimental constant, and ω_p is the velocity of the propeller. Some simple experimental results show that the quadratic approximation is reliable [24]. From this model, thrusters are locally fedback by the use of a velocity sensor, associated to each propeller, in order to obtain the propeller velocity that corresponds to the required thrust. There are more advance and precise thruster models [8, 29]. Nevertheless, they require a better dynamic thruster characterization than that made at the time of these experiments.

Finally, the computational effort required by the real-time electronics architecture of the vehicle depends on the control equations, as well as the detail structure of the fuzzy estimators, described in the next section. Thus, supposing that the fuzzification process needs for each membership function, one sum and one float point multiplication, and that the buoyancy of the vehicle is neutral, the computational effort per sample period for the PI, SM and AFSM controllers, and the three controllable DOF, can be seen in Table 4.

Based on the number of float point sums and multiplications of Table 4, we can conclude that despite the number being significantly larger for the case of the AFSM, the proposed controller is easy to implement in the electronic architecture of the Snorkel vehicle with a sample time of 100 ms.

4.3 Definition of Control Parameters

Before starting with the tests, it is necessary to fix in a reasonable way the values of the parameters which form part of the controllers, from the vehicle model and its degree of uncertainty. Firstly, a reference model, implemented by a first order Butterworth low past filter, has been introduced to smooth the velocity references, trying to obtain a reasonable

Table 4 Computational effort

Float pint operations	MULT	SUM
PI	6	9
SM	45	36
AFSM	165	254

Table 5 Reference model. Butterwort filter time constant

DOF	Surge	Heave	Yaw
Time constant (s)	1,66	3,33	1,66

control effort. Its time constant is equal to the smaller time constant of the vehicle for each DOF, and can be seen in Table 5.

In the case of the PI controller, its parameters K_{pi} and K_{ii} have been fixed by identification with the sliding mode control constants. To make this identification, the term $f_i(\xi)$ and the saturation function have been eliminated from the control law. This means,

$$K_{pi} = \frac{\lambda_i + \eta_{\Delta i} \cdot b_i}{g_i(\xi)}, \qquad K_{ii} = \frac{\lambda_i \cdot \eta_{\Delta i} \cdot b_i}{g_i(\xi)} \qquad (16)$$

Several parameters have to be fixed by the sliding control. From the objective of not having the system under great control efforts, selected values for time constants of the sliding ($1/\lambda_i$) and approaching (T_i) phase will be two times larger than the natural time constants of the system. Additionally, to fix the value of $\eta_{\Delta i}$ based on Eq. 9, the maximum value of the uncertainty of the functions $f_i(\xi)$, $g_i(\xi)$ and d_i, must be established and the initial value of the sliding surface s_{0i} [25]. For the case of $f_i(\xi)$ and $g_i(\xi)$ this uncertainty will vary around ±20%, while for the case of d_i, it will take a maximum value of the 20% of the $f_i(\xi)$. Lastly, the thickness of the boundary layer, b_i, has to be defined. For its determination, numerical simulations have been developed, increasing as much as possible its value, and trying to avoid oscillations in the estimation process. As a summary, in Table 6 the values of parameters for the SM and PI controllers are shown.

In order to define fuzzy estimators, firstly it is necessary to fix which of the kinematic variables are used for each estimator. To make this kind of decision, knowledge of the variables which determine dynamics of each DOF has to be taken into account. This partial knowledge of the dynamics can be obtained from the model of the vehicle, as in the case of this research, or from the a priori knowledge that an operator possesses. From here, it has been decided to take the relations of Table 7, where $\mu_{Ai}(k)$ are the membership functions of the k variable and the dependence of $\widehat{g}_i(\xi)$ with respect to the velocity of each DOF allows us to keep the adaptation process active and to absorb the gain variation of the propulsion system depending on this velocity.

In addition to this, it is necessary to define the membership functions of each fuzzy variable. This means to determine the number, the kind and the parameters of the membership functions. The membership functions chosen for this application have a Gaussian form, in which the centre and the typical deviation are the most relevant parameters. A different number of membership functions have been used, depending on the precision required in the adjustment. In a general manner, five membership functions will be used in the estimation of the $\widehat{f}_i(\xi)$ functions, for the variable to be controlled and three in any other case. In Table 8, the numerical values associated to each membership function

Table 6 PI and sliding control parameters

DOF	K_i	K_p	λ	μ_Δ	B
Surge	56.42	212.85	0.3	0.38	6
Heave	26.44	210.18	0.15	0.13	6
Yaw	3.13	13.68	0.3	0.55	1.75

Table 7 Fuzzy estimator's parameters

DOF	$f(\zeta)$	$g(\zeta)$	M_f	M_g	ε	r_1	r_2
Surge	$\mu_{A_1}(\dot{x}_u), \mu_A(\dot{x}_v), \mu_{A_2}(\dot{x}_r)$	$\mu_{A_2}(\dot{x}_u)$	0.36·2	0.012·2	0.012/2	0.2	0.005
Heave	$\mu_{A_1}(\dot{x}_w)$	$\mu_{A_2}(\dot{x}_w)$	0.13·2	0.0044·2	0.0044/2	0.2	0.01
Yaw	$\mu_{A_1}(\dot{x}_r), \mu_{A_2}(\dot{x}_u), \mu_A(\dot{x}_v)$	$\mu_{A_1}(\dot{x}_r)$	0.53·2	0.0177·2	0.0177/2	10	0.005

can be seen. The objective followed, in order to fix these values, is to cover all the dynamic range of the variables, so as to achieve an overlap of the nearby membership functions.

Other specific parameters of the fuzzy estimators are related to the adjustment function of the output consequents. The maximum value of these parameters is determined by the constants M_{fi} and M_{gi}, of which a value has been fixed following the criteria of doubling the theoretical values of $\hat{f}_i(\xi)$ and $\hat{g}_i(\xi)$ functions [25]. Additionally, the criterion chosen to fix the values of ϵ_i is to multiply the same theoretical value of $\hat{g}_i(\xi)$ by 1/2. From this, it can be extracted that the system is capable of absorbing perturbations and variations of the vehicle model and parameters, according to this criteria.

Also, it is necessary to determine the constants that establish the adaptation velocities. In this case, these constants have been fixed by data analysis of numerical simulations, meeting a compromise between velocity and oscillation in the adaptation process. As a summary, Table 7 shows the group of parameters associated to the adaptation of the weight of the output consequents.

One of the considerations to have in mind, for the correct interpretation of the tests, is that the $\hat{f}_i(\xi)$ functions have void initial values, or equally the values of the θ_{fi} parameters are zero. This allows us to demonstrate the capability of the system in the adaptation process, in spite of the lack in the tracking performance of the input references at the start of the test. The estimators of the $\hat{g}_i(\xi)$ functions take as initial values the theoretical ones, from the Snorkel vehicle model [25], Table 9.

5 Experimental Results

This section reports a comparative experimental evaluation of the tracking performance of the controllers previously described. The tests investigate the adaptation capabilities of the AFSM controller, and the effect of model accuracy, noise in the measurement of kinematic variables and thruster saturation on controller performance.

Table 8 Description of membership functions

Variable	Centre membership functions	Typical deviation
$\mu_{A_1}(\dot{x}_u)$	[−0.5 −0.25 0 0.25 0.5] m/s	0.125 m/s
$\mu_{A_2}(\dot{x}_u)$	[−0.5 0 0.5] m/sec	0.25 m/s
$\mu_A(\dot{x}_v)$	[−0.3 0 0.3] m/s	0.15 m/s
$\mu_{A_1}(\dot{x}_w)$	[−0.3 −0.15 0 0.15 0.3] m/s	0.075 m/s
$\mu_{A_2}(\dot{x}_w)$	[−0.3 0 0.3] m/s	0.15 m/s
$\mu_{A_1}(\dot{x}_r)$	[−0.7 −0.35 0 0.35 0.7] rad/s	0.175 rad/s
$\mu_{A_1}(\dot{x}_r)$	[−0.7 0 0.7] rad/s	0.35 rad/s

Table 9 Initial values of θ_{fi} and θ_{gi}

DOF	$\boldsymbol{\theta}_f^T$	$\boldsymbol{\theta}_g^T$
Surge	$[0.. \ 0]_{45 \times 1}$	[0.012 0.012 0.012]
Heave	$[0.. \ 0]_{5 \times 1}$	[0.0044 0.0044 0.0044]
Yaw	$[0.. \ 0]_{45 \times 1}$	[0.0177 0.0177 0.0177]

Table 10 shows the parameters of the body frame references, used to carry out the experiments. The oscillatory shape permits us to keep the estimation process active. These input references have square and triangular forms, because these types of forms contain different spectra components. In this way, the behaviour of the system is analysed for various frequencies at the same time versus the use of a sinusoidal signal, avoiding particular frequency effects and improving the validity of the results.

Some norms to quantitatively compare the performance of each controller have been adopted. A position error norm for each DOF is calculated as $\tilde{x} = \text{mean}(|x_d - x|)$. The velocity error norm is calculated as $\tilde{\dot{x}} = \text{mean}(|\dot{x}_d - \dot{x}|)$, and finally the control effort norm of the corresponding active thruster in each test is calculated as $\tau_{\text{TOTAL}} = \text{mean}(|\tau_d|)$.

5.1 Comparative Performance with Velocity Reference and Model Adaptation Capabilities

The first section reports a direct comparison of the PI, SM and AFSM controllers performance, as well as the control effort of each controller, while a yaw velocity reference is tracked, Table 10. Additionally it attempts to show the performance of the AFSM controller to estimate vehicle dynamics, from the fact that a priori vehicle model is purely theoretical. In order to implement the control law, and based on Snorkel sensorial system, it has to be emphasized that the real position and position reference are obtain directly by integrating the real velocity and velocity reference respectively. This will mean a problem of drift in the estimation of the vehicle angular position, but based on vehicle architecture, an angular error is irrelevant, because the guidance controller is in charge of local position tracking.

From an analysis of the Fig. 6c we observe that the tracking of the input reference for the AFSM controller is nearly perfect, always with a reasonable control effort, Fig. 6c (bottom), in spite of the oscillatory behaviour when the output value is close to zero. The oscillation can be caused by an error in the on line algorithm that makes null the offset of the gyroscope signals. The figures correspond to the period after the initial adaptation process of $\widehat{f}_r(\boldsymbol{\xi})$ and $\widehat{g}_r(\boldsymbol{\xi})$ functions, supposing that these have reached their optimal values.

From the beginning of the test, the estimation of the $\widehat{f}_r(\boldsymbol{\xi})$ function, Fig. 7 (top), is stable during the entire test in spite of the peaks, whose origin is the oscillation of the system output described before. Similarly, the estimation of the $\widehat{g}_r(\boldsymbol{\xi})$ function reaches its stable value over the minimum established, Fig. 7(bottom). The appearance of oscillations in these

Table 10 References

| Reference	Amplitude	Offset	Frequency (Hz)	Period (s)
Yaw velocity	10°/s	0°/s	0.025	40
Yaw	50°	70°	0.025	40
Depth	0.3 m	0.7 m	0.025	40

Fig. 6 a Plot of PI controller in the yaw DOF. (*Top*) Actual yaw velocity $\dot{x}_r$(- -) and reference $\dot{x}_{rd}$(–). (*Medium*) Velocity tracking error. (*Bottom*) Thrust of a horizontal thruster. **b** Plot of SM controller in the yaw DOF. (*Top*) actual yaw velocity $\dot{x}_r$(- -) and reference $\dot{x}_{rd}$(–). (*Medium*) Velocity tracking error. (*Bottom*) Thrust of a horizontal thruster. **c** Plot of AFSM controller in the yaw DOF. (*Top*) actual yaw velocity $\dot{x}_r$(- -) and reference $\dot{x}_{rd}$(–). (*Medium*) Velocity tracking error. (*Bottom*) Thrust of a horizontal thruster
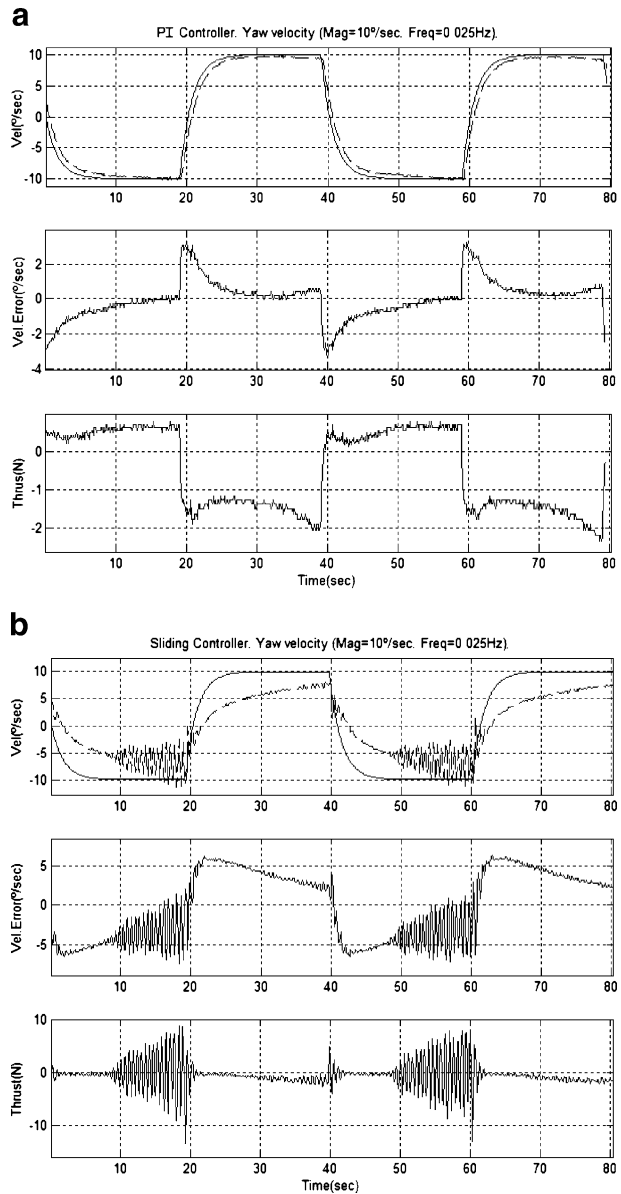
functions attempts to make null the value of the sliding surface in the quickest method possible.

Figure 6a and b show the tracking error and the control effort of the PI and SM controllers, using the same input reference as in the case of the AFSM controller. It can be easily observed that the PI controller presents a worse performance and the SM controller even worse than the AFSM controller. In the case of the SM controller test, the existence of large chartering when yaw velocity takes negative values is caused by an error in the

Fig. 6 (continued)
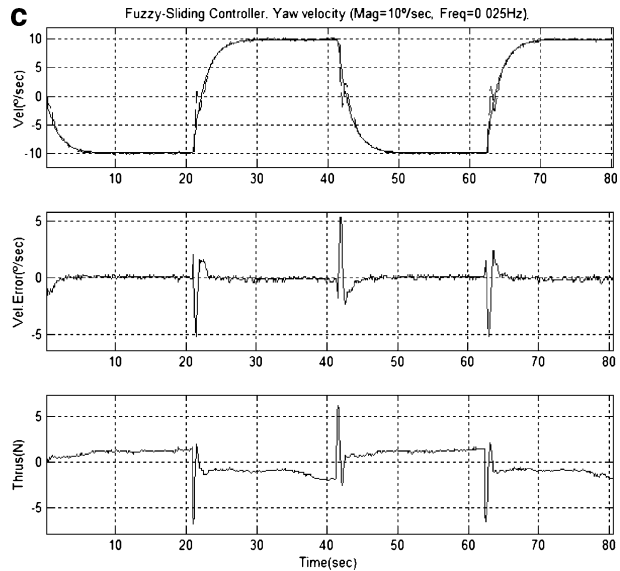
implementation of the control algorithm. In Figs. 8 and 9, this comparison is made analytically, using a square and a triangular reference respectively. They conclude that AFSM controller presents the smaller velocity error, while its control effort is only slightly higher than the control effort of the PI controller. This is due to the adaptation capabilities of the AFSM controller, based on its fuzzy estimators and the right adaptation law. The performance of a model based controller, as the SM controller, depends entirely on the accuracy of the dynamic plant model used in the designing of the controller. This section also corroborates the lack of accuracy of the theoretical determined dynamical plant model for the Snorkel UUV, presented in Section 2.

5.2 Effect of Thruster Saturation with Position Reference

The second set of tests reports a direct comparison of the PI, SM and AFSM controller performance, while tracking a position input reference for the yaw angle, Table 10. Nevertheless, this controller will use velocity references as input, as is required by the vehicles architecture. Additionally, it attempts to show the influence of thruster saturation in the velocity and positions tracking errors. In this test, velocity reference is the derivative of the angular reference.

It is evident that there are some deficits in the tracking of the input position and velocity references, for the case of the AFSM controller, Figs. 10 and 11. Nevertheless, the final values of the yaw angle and velocities are reached, in spite of the appearance of overshoot. The excessively fast and large velocity reference generates fast and high thrust references, Fig. 12 (top), which cause high turn velocity in the propellers of the horizontal thrusters, Fig. 12 (bottom). The velocity reference of the propellers is achieved by the thrust controller, but in spite of that, and by using real data of the propulsion system [23], it can be supposed that the hydrodynamic part of the propulsion system is not as fast as it must be, saturating the thrusters.
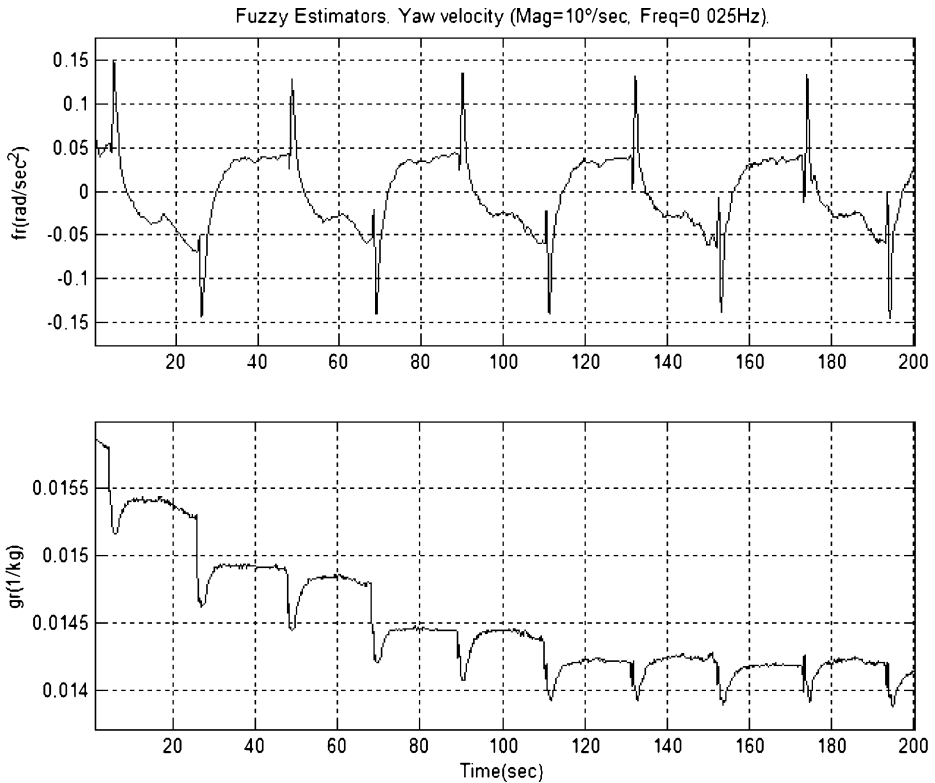
Fig. 7 Plot of FASM controller in the yaw DOF. (*Top*) Evolution of $\widehat{f}_r(\xi)$. (*Bottom*) Evolution of $\widehat{g}_r(\xi)$

Figures 13 and 14 directly show the comparison among the PI, SM and AFSM controllers, using the same square and triangular reference. It can be concluded that PI controller presents the smaller velocity and angle tracking errors, as well as slightly smaller control effort than the AFSM controller. This advantage is due to its better performance under the saturation of the thrusters. Thrusters saturation represents an unmodeled discontinuous dynamic [27], and can be affirmed that this has a greater negative effect on

Fig. 8 Plot of velocity tracking error (*black*) and control effort (*grey*) for PI, SM and AFSM controllers. Square reference, amplitude 10°/s, frequency 0.025 Hz. $\widetilde{x} = \mathrm{mean}\left(\left|\dot{x}_d - \dot{x}\right|\right)$ [°/s] and $\tau_{\mathrm{TOTAL}} \geq = \mathrm{mean}(|\tau_d|)[N]$
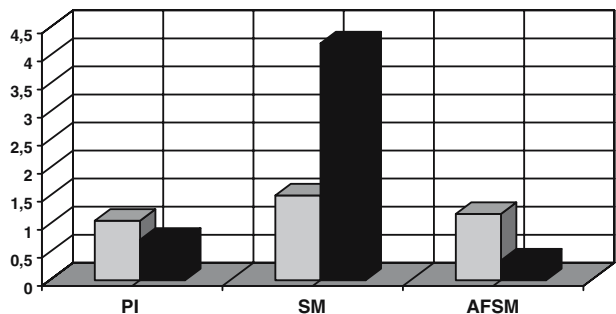
Fig. 9 Plot of velocity tracking error (*black*) and control effort (*grey*) for PI, SM and AFSM controllers. Triangular reference, amplitude 10°/s, frequency 0.025 Hz. $\tilde{x} = \text{mean}(|\dot{x}_d - \dot{x}|)$ [°/s] and $\tau_{\text{TOTAL}} = \text{mean}(|\tau_d|)$[N]
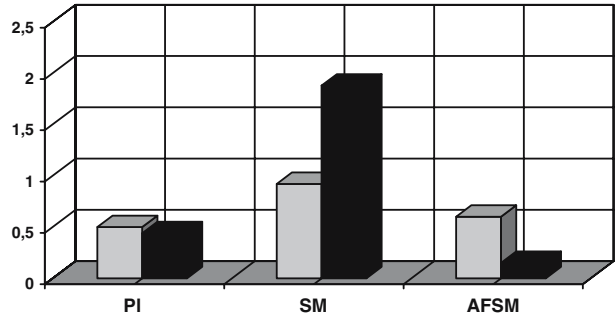
the adaptive controllers, because while they are not only based on an inaccurate model structure, as the SM controller, the AFSM attempts to estimate the parameter values of that ill-structured plant model. Thus, future work must be done in dealing with handling adaptation to actuators saturation [22]. Again, the performance of the SM controller is justified due to the lack of the theoretical model of the Snorkel vehicle.
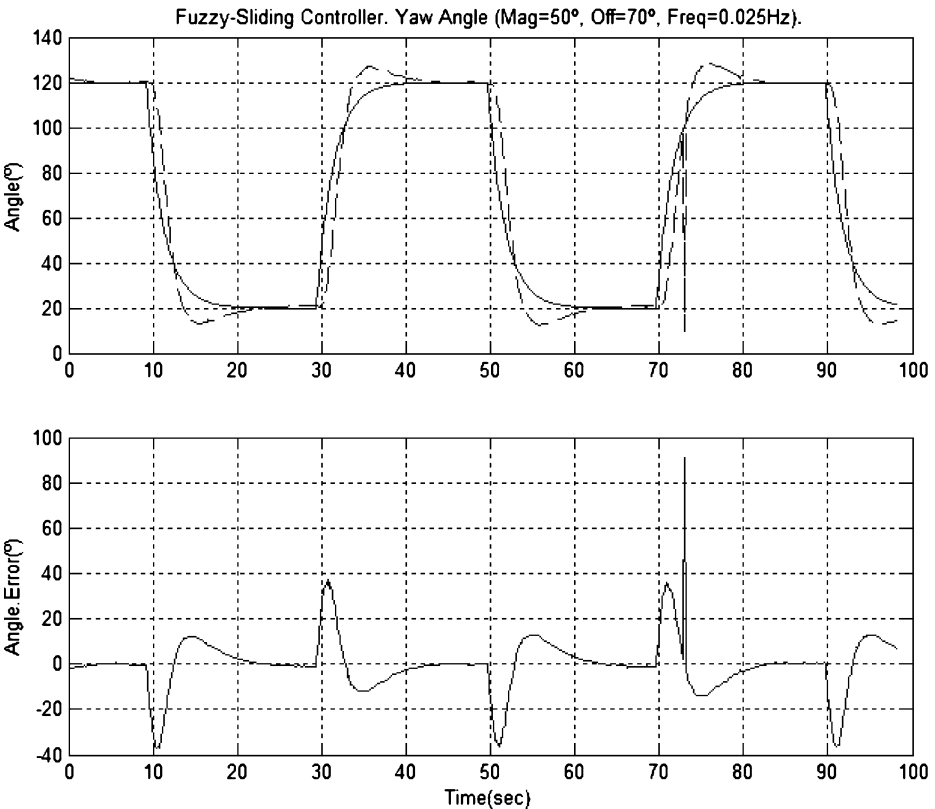
Fig. 10 Plot of AFSM controller in the yaw DOF. (*Top*) actual yaw angle x_r (- -) and reference x_{rd} (–). (*Bottom*) Yaw angle tracking error
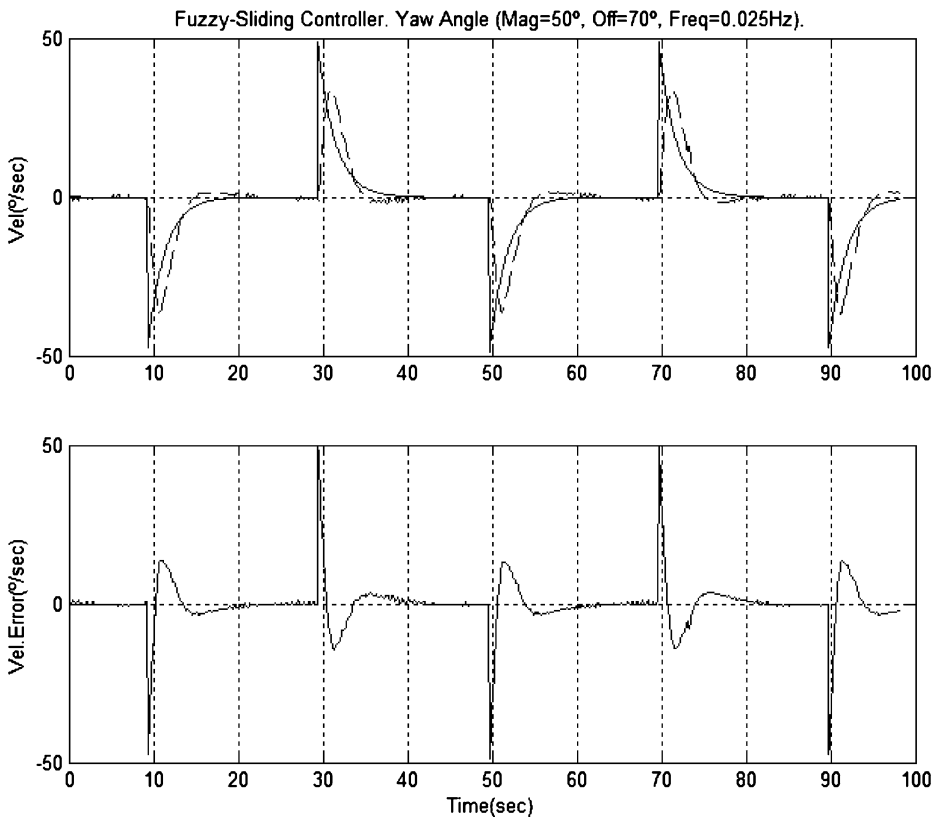
Fig. 11 Plot of AFSM controller in the yaw DOF. (*Top*) actual yaw velocity $\dot{x}_r$ (-.-) and reference $\dot{x}_{rd}$ (–). (*Bottom*) Yaw velocity tracking error

5.3 Model Adaptation Capabilities and Noise in Kinematic Measurements

The last section attempts to show the performance of the controllers PI, SM and AFSM, while tracking the square depth position reference of Table 10, and in the presence of a change in the buoyancy of the vehicle, not previously considered in the vehicle model. Additionally, and contrary to the previous tests, there is a high noise level associated with the measurements of vehicle depth and heave velocity, Table 2. Again heave velocity reference is the derivative of the depth reference.

In Fig. 15, the better performance of the AFSM controller (Bottom) can be observed. This control technique is capable of reaching the permanent regime of input reference, while the other control techniques are not able to do it. Despite this, the transitory response does not track the reference due to two different reasons: the high quantification noise level associated with the measurements of depth and heave velocity, and the high rates of depth reference that at the same time generate high values of velocity references, that can not be followed by the propulsion system [24], Fig. 16 (Top). A possible solution to this problem is to obtain the position references from the integration of velocity references, which could be saturated to reasonable values for the propulsion system.
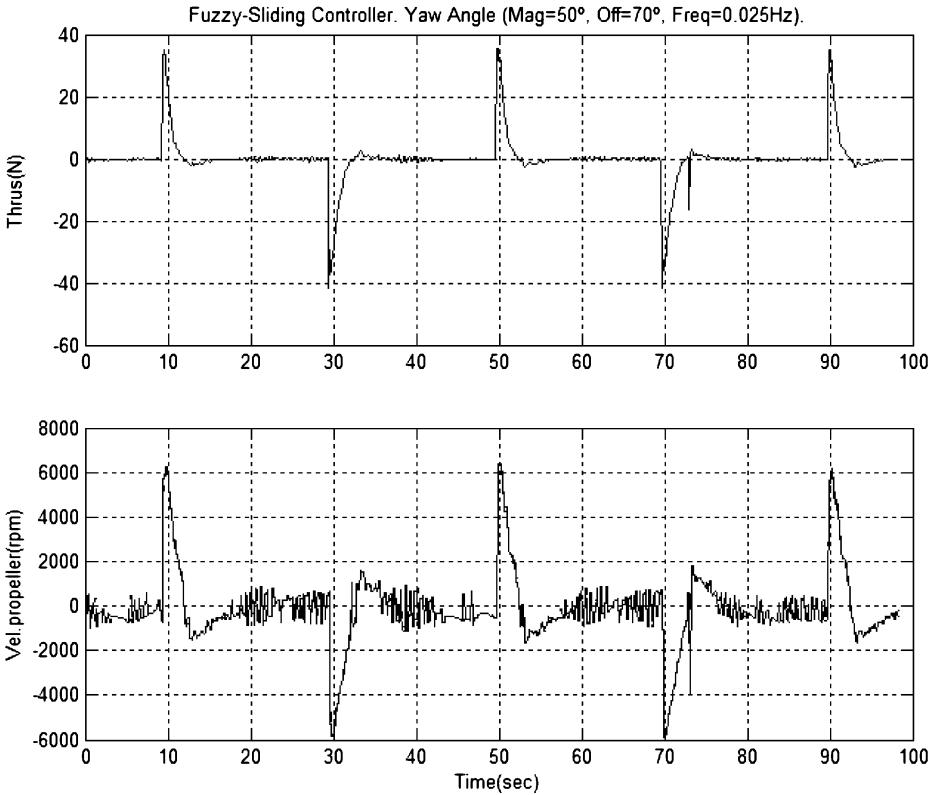
Fig. 12 Plot of AFSM controller in the yaw DOF. (*Top*)Thrust reference of the horizontal thruster. (*Bottom*) Propeller reference $\omega_{pd}(-)$ and actual ω_p (- -) velocity of the same thruster

This better performance of the AFSM controller is based on the adaptation capability of the controller. Thus, during the development of this test the vehicle buoyancy was too negative, and its value had not been considered in vehicle model. Only a control law with estimation capabilities of $\widehat{f_w}(\xi)$, Fig. 16 (Bottom), can absorb the uncertainty. Again, the results presented in this section clearly indicate that the tracking performance of the SM controller is dependent on the accuracy of the model, as in this case the vehicle buoyancy
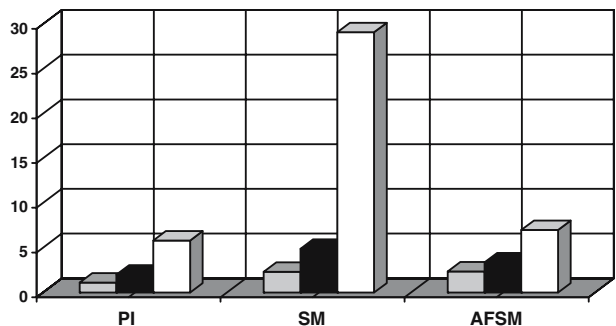
Fig. 13 Plot of angle tracking error (*white*), velocity tracking error (*black*) and control effort (*grey*) for PI, SM and AFSM controllers. Square reference, amplitude 50°, offset 70°, frequency 0.025 Hz. $\tilde{x} = \text{mean}$ $\left(\left|x_d - x\right|\right)$ [°], $\tilde{\dot{x}} = \text{mean}$ $\left(\left|\dot{x}_d - \dot{x}\right|\right)$[°/s] and $\tau_{\text{TOTAL}} = \text{mean}(|\tau_d|)$[N]

Fig. 14 Plot of angle tracking error (*white*), velocity tracking error (*black*) and control effort (*grey*) for PI, SM and AFSM controllers. Triangular reference, amplitude 50°, offset 70°, frequency 0.025 Hz. $\widetilde{x} = \text{mean}\left(\left|x_d - x\right|\right)[°]$, $\widetilde{\dot{x}} = \text{mean}\left(\left|\dot{x}_d - \dot{x}\right|\right)[°/s]$ and $\tau_{\text{TOTAL}} = \text{mean}(|\tau_d|)[N]$
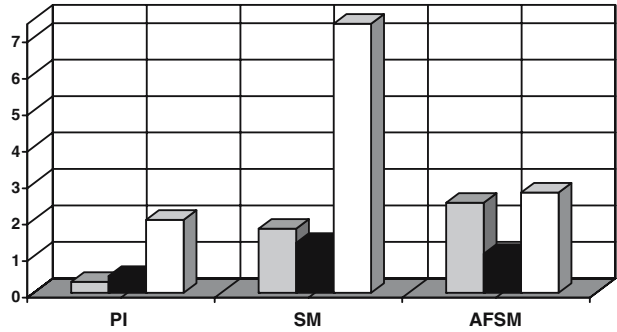
was not considered, the SM controller behaves poorly. Thus, we can conclude that a bigger effort must be made in the SM controller design and the vehicle model identification in order to accomplish a good enough performance with the SM controller.
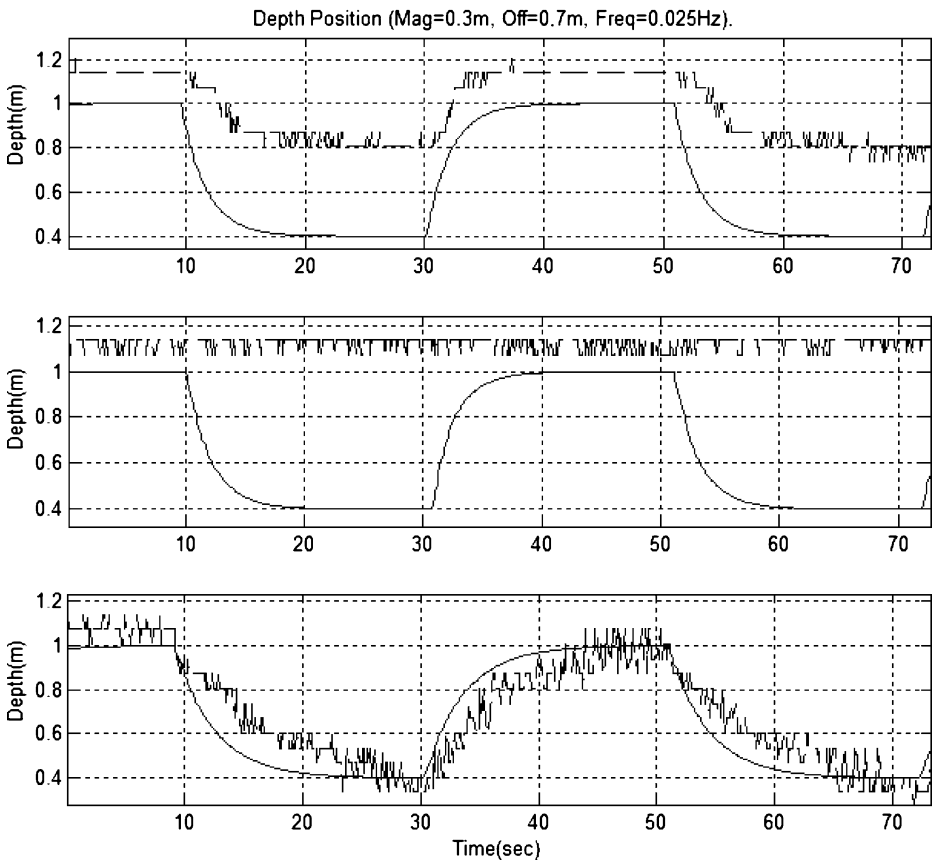
Fig. 15 Plot of actual depth x_w (- -) and reference x_{wd} (–) for (*Top*) PI controller, (*Medium*) SM controller and (*Bottom*) AFSM controller. Square reference, amplitude 0.3 m, offset 0.4 m, frequency 0.025 Hz
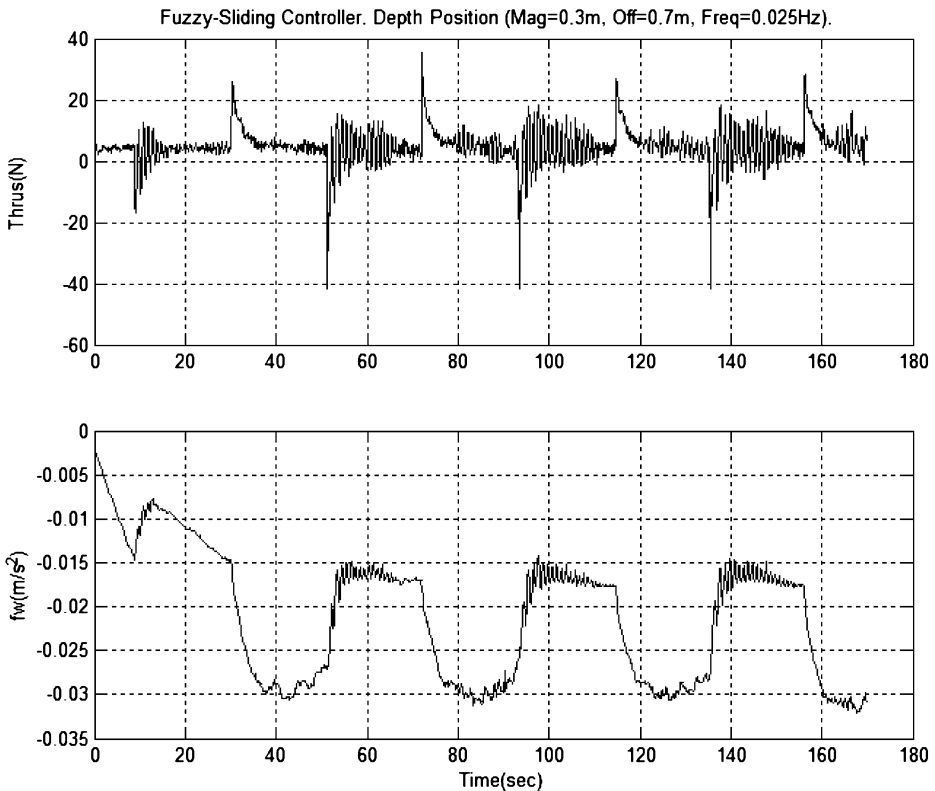
Fig. 16 Plot of AFSM controller in the heave DOF. (*Top*) Thrust reference of the vertical thrusters. (*Bottom*) Evolution of $\widehat{f}_w(\xi)$

6 Conclusions

This paper reports a preliminary experimental evaluation of the adaptive fuzzy sliding mode (AFSM) controller for the kinematic variables of an underactuated underwater vehicle manoeuvred at low-speed. The proposed controller is part of a guidance and control architecture, and it abstracts the dynamics of the vehicle to the guidance controller, giving a dynamic behaviour similar to the reference model. Thus, the kinematic controller receives as inputs, from the guidance system, the surge and yaw velocity, and the heave position. The AFSM controller, applied for the very first time in a UUV, allows us to consider the non-linearity of the system without having to appeal to linearization, which in a system with a great number of DOF is a tedious process and without warranties of stability. Also, it is capable of adapting to uncertainty in the model parameters and in the model itself. This feature permits the designer to avoid a tedious process of model parameter identification, helping to reduce the design cost of the vehicle.

The theoretical and practical stability of the AFSM controller has been shown, assuring the convergence of the system to the input references, with a reasonable control effort and a minimum knowledge of the model and parameters of the vehicle. The controller is capable of incorporating and compensating the dynamic problems and the perturbations of underwater vehicles. Also, it generates systems that are simple to implement and interpret.

From a theoretical point of view, the proposed controller could be defined as a combination of an adaptive and robust system. In this way, it presents the advantages of robust control like the capability of adapting to rapid variation of the parameters, perturbations, noise from unmodeled dynamics, and theoretical insensibility to errors of the state measurements and its derivatives. And also, it presents the advantages of adaptive systems, like no requirement for prior and precise knowledge of uncertainty, reducing the required knowledge of system boundaries of uncertainty, and the capacity of improving the output performance as the system adapts.

The fuzzy adaptive part of the controller permits us to relax the design conditions of the sliding part, due to perturbations and variation in model parameters which are compensated and adapted by the fuzzy part of the system. This permits us to decrease the oscillations demanded from the propulsion system, which are caused by the high discontinuous gain existing in pure sliding systems.

One of the restrictions of the fuzzy adaptive part is the low speed of the parametric adjustment, despite the fact that in underwater vehicles this is not usually important. The adaptation velocity depends on the values of some constants, so that as their values increase the overshoot also increases. Nevertheless, this lack does not have a special relevance in the system due to the fact that it is compensated by the sliding part of the controller.

In order to carry out the tests the simple case semi-decoupled plant model has been considered employing thrust input, constant added mass, constant square drag and constant buoyancy. We have compared the performance of the proposed controller with the very used PI controller and a simple model based SM controller. The experiments of the close-loop performance of these systems corroborate the theoretical predictions. Moreover, the experiments suggest that the AFSM controller is a valid method to be applied in underwater vehicles that outperform the PI and SM controllers using velocity trajectories. Thruster saturation significantly degrades the performance of AFSM controller, while PI controller shows better performance under this circumstance. The success of a simple model based SM controller relies on the plant model parameters to be exactly correct, where as AFSM, based on its adaptation capabilities, is not affected by inaccuracy in theoretical plant model. Noise is another factor that significantly affects the performance of the SM controller, and less seriously of the AFSM controller.

In the AFSM controller, the simultaneous estimation of the $\widehat{f}(\xi)$ and $\widehat{g}(\xi)$ functions, can cause the true values of these functions not to be achieved, but a solution that makes zero the value of the sliding surface as soon as possible, which is close to the optimal value. The evolution of both functions is conditioned by the adaptation velocities. The fuzzy estimators of the $\widehat{g}(\xi)$ functions permit us to absorb the uncertainty associated with the evolution of the gain of the propulsion system, compensating the unmodeled influence that the vehicle velocities have on the real thrust. Also, they absorb parameter variation such us mass, inertia moments and centre of mass position.

A future work to be developed is to carry out control tests of the kinematic variables with combined input references, but in order to do that it is necessary to get rid of the restrictions of the water tank. In the same way, tests associated with the guidance control system, considering external perturbations like water currents, will be made. To be able to perform the guidance control, it is necessary to design the navigation algorithms based on the FLS images that permit us to obtain the values of the trajectory tracking errors.

References

1. Aguilar, L.E., Souères, P., Courdesses, M., Fleury, S.: Robust path following control with exponential stability for mobile robots. Paper presented at IEEE international conference on robotics and automation, pp. 3279–3284, Leuven, Belgium, 1998
2. Aicardi, M., Casalino, G., Indiveri, G., Aguilar, A., Encarnacao, P., Pascoal, A.: A planar path following controller for underactuated marine vehicles. Paper presented at Mediterranean conference of control and automation, Dubrovnick, Croatia, 2001
3. Antonelli, G., Chiaverini, S., Sarkar, N., West, M.: Adaptive control of and autonomous underwater vehicle: Experimental results on ODIN. Paper presented at IEEE international symposium in computational intelligence in robotics and automation, Monterrey, CA, 1999
4. Antonelli, G., Chiaverini, S., Sarkar, N., West, M.: Adaptive control of and autonomous underwater vehicle: experimental results on ODIN. IEEE Trans. Control Syst. Technol. **9**, 756–765 (2001)
5. Antonelli, G. (ed.): Underwater Robots. Motion and Force Control of Vehicle-manipulator Systems. In: Springer Tracts in Advanced Robotics, Napoli, Italy (2002)
6. Antonelli, G., Caccavale, F., Chiaverini, S., Fusco, G.: A novel adaptive control law for underwater vehicles. IEEE Trans. Control Syst. Technol. **11**(2), 109–120 (2003)
7. Arimoto, S., Miyazaki, F.: Stability and robustness of PID feedback control for robot manipulators of sensory capabilities. Paper presented at robotics research, first int. symp, Cambridge, MA, 1984
8. Bachmayer, R., Whitcomb, L.: Adaptive parameter identification of an accurate non-linear model for marine thruster. J. Dyn. Syst. Meas. Control **2**, 125–131 (2002)
9. Choi, S.K., Yuh, J.: Experimental study on a learning control system with bound estimation for underwater vehicles. International Journal of Autonomous Robots **3**(2/3), 187–194 (1996)
10. Cristi, R., Papoulias, F.A., Healey, A.: Adaptive sliding control mode of autonomous underwater vehicles in the dive plane. IEEE J. Oceanic Eng. **15**(3), 462–470 (1991)
11. DeBitetto, P.A.: Fuzzy logic for depth control for unmanned undersea vehicles. Paper presented at symposium of autonomous underwater vehicle technology, Cambridge, MA, 1994
12. Encarnacao, P.: Non-linear path following control systems for ocean vehicles. Dissertation, Universidad Técnica de Lisboa, Instituto Superior Técnico, Lisbon (2002)
13. Espinosa, F., López, E., Mateos, R., Mazo, M., García, R.: Application of advanced digital control techniques to the drive and trajectory tracking systems of a wheelchair for the disabled. Paper presented at emerging technologies and factory automation, Barcelona, 1999
14. Fossen, T.I. (ed.): Underwater Vehicle Dynamics. Wiley, Chichester (1994)
15. Fossen, T.I., Fjellstad, O.E.: Robust adaptive control of underwater vehicles: a comparative study. Paper presented at IFAC workshop on control applications in marine systems, Trondhein, Norway, 1995
16. Fossen, T.I., Paulsen, M.: Adaptive feedback linearization applied to steering of ships. Paper presented at 1st IEEE conference on control applications, Dayton, Ohio, 1991
17. Gee, S.S., Hang, C.C., Zhang, T.: A direct method for robust adaptive non-linear with guaranteed transient performance. Syst. Control. Lett. **37**, 275–284 (1999)
18. Goheen, K.G., Jefferys, E.R.: On the adaptive control of remotely operated underwater vehicles. Int. J. Adapt. Control Signal Process. **4**(4), 287–297 (1990)
19. Healey, A.J., Lienard, D.: Multivariable sliding mode control for autonomous diving. IEEE J. Oceanic Eng. **18**, 327–339 (1993)
20. Hsu, L., Costa, R.R., Lizaralde, F., Cunha da, J.P.V.S.: Dynamic positioning of remotely operated underwater vehicles. IEEE Robot Autom. Mag. **7**, 21–31 (2000)
21. Indiveri, G.H., Aicardi, M., Casalino, A.: Non-linear time-invariant feedback control of an underactuated marine vehicle along a straight course. Paper presented at IFAC conference on manoeuvring and control of marine craft. Aalborg, Denmark, 2000
22. Johnson, E.N., Calise, A.J.: Pseudo-control hedging: a new method for adaptive control. Paper presented at workshop on advances in guidance and control technology, Redstone Arsenal, AL, 2000
23. Koivo, H.N.: A multivariable self-tuning controller. Automatica **16**(4), 351–366 (1980)
24. Manfredi, J.A., Sebastián, E., Gomez-Elvira, J., Martín, J., Torres, J.: Snorkel: Vehículo subacuático para la exploración del Río Tinto. Paper presented at XXII Jornadas de Automática, Barcelona, 2001
25. Sebastián, E.: Control y navegación semi-autónoma de un robot subacuático para la inspección de entornos desconocidos. Dissertation, Universidad de Alcalá, Alcalá de Henares, Madrid (2005)
26. Slotine, J.J., Li, W. (eds.): Applied Non-linear Control. Prentice-Hall, Englewood Cliffs, NJ (1991)
27. Smallwood, D.A., Whitcomb, L.L.: Model-based dynamic positioning of underwater robotic vehicles: theory and experiment. IEEE J. Oceanic Eng. **29**(1), 169–186 (2004)
28. Vaganay, J., Bellingham, J., Leonard, J.: Outlier rejection for autonomous acoustic navigation. Paper presented at IEEE International conference on Robotics and Automation, Minneapolis, 1996

29. Whitcomb, L., Yoeger, D.: Preliminary experiment in the model-based thrusters control for underwater vehicle positioning. IEEE J. Oceanic Eng. **15**(3), (1999)
30. Wang, L.X. (ed.): Adaptive Fuzzy Systems and Control. Prentice-Hall, Englewood Cliff, NJ (1994)
31. Wang, J., Get, S.S., Lee, T.H.: Adaptive fuzzy sliding mode control of a class of non-linear systems. Paper presented at 3rd Asian control conference, Shanghai, 2000
32. Yoerger, D.R., Slotine, J.J.: Adaptive sliding control of an experimental underwater vehicle. Paper presented at IEEE international conference on robotics and automation, 1991
33. Yoerger, D.R., Slotine, J.J.: Robust trajectory control of underwater vehicles. IEEE J. Oceanic Eng. **10** (4), 462–470 (1985)
34. Yuh, J.: Learning control for underwater robotics vehicles. IEEE Control Syst. Mag. **14**(2), 39–46 (1994)
35. Yuh, J.: Design and control of autonomous underwater robots: a survey. Auton. Robots **8**, 7–24 (2000)